

Synthesis, molecular docking studies, and in vitro screening of barbiturates/thiobarbiturates as antibacterial and cholinesterase inhibitors

Saira Mumtaz · Rashad Hussain · Abdul Rauf ·
M. Q. Fatmi · H. Bokhari · M. Oelgemöller ·
A. M. Qureshi

Received: 9 July 2013 / Accepted: 14 October 2013
© Springer Science+Business Media New York 2013

Abstract On the basis of observed biological activity of barbiturates/thiobarbiturates, a set of 13 hydrazinecarboxamide/hydrazinecarbothioamides derivatives were designed and synthesized in good to excellent yield with extensive structural characterization. These compounds were screened for antibacterial and cholinesterase inhibitory activities. Two of the compounds **1** and **2** showed moderate bactericidal activity. Compounds **10** and **4** were found to be the most active *acetyl/butryl cholinesterase* inhibitor, respectively (AChEI; **10**; $IC_{50} = 40.78 \mu\text{M}$ and BChEI; **4**; $IC_{50} = 3.31 \mu\text{M}$). In silico molecular docking studies were carried out to identify active interacting sites of drug and enzyme and to establish structure–activity relationships. When predicted cholinesterase binding energies were compared with the experimentally determined inhibitory concentrations (IC_{50}), most active compounds were also found to be the most favorable for binding. The binding scores of compounds **10** and **4** were -10.2 and -9.3 kcal/mol, respectively.

Keywords Thiobarbituric acid · Thiosemicarbazone · Hydrazinecarboxamide/hydrazinecarbothioamides · Molecular modeling · *Acetyl cholinesterase* · *Butryl cholinesterase*

Introduction

One of the most desirable and excruciating process, in pharmacy, is to develop new drugs with potential therapeutic applications. Recent technological advancements in computational biology/chemistry have made possible that the rational drug designing become more viable and less tedious. For the target-oriented drug synthesis, mechanism of action at molecular level is required. Molecular modeling is one of the computational tools that can assist chemists by establishing such structure activity relationships (SAR).

Molecular modeling gives valuable insight into the mode of action of barbituric acid derivatives as hypnotic, sedative, anti-urease, and antiepileptic therapeutic drugs (Khan *et al.*, 2011; Mihai *et al.*, 2008). HIV-1 protease inhibition by barbiturates was also subjected to predict new active pharmacophores (Santos-Filho and Hopfinger, 2006; Andrade *et al.*, 2010; Pan *et al.*, 2003).

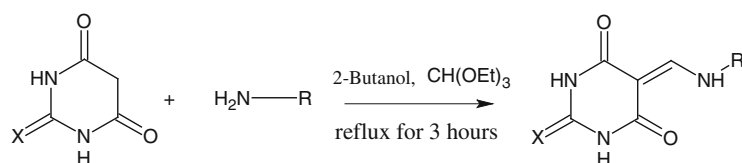
Moreover barbiturates are found to be active against cholinesterase. On the account of their behavior and specificity to inhibitors, animal cholinesterase is classified into *acetyl cholinesterase* (AChE) and *butryl cholinesterase* (BChE). Basically, AChE and BChE hydrolyzes two different classes of choline, i.e., acetylcholine and butrylcholine (Chatonnet and Lockridge, 1989; Ryhänen, 1983; Ekholm, 2001). Besides sharing 65 % homology in amino acid sequence, AChE and BChE, are encoded by the corresponding genes located on different chromosomes. The active center of AChE mainly consists of esteric site and

S. Mumtaz · A. M. Qureshi (✉)
Institute of Chemical Sciences, Bahauddin Zakariya University,
Multan 60800, Pakistan
e-mail: shamashfaq@yahoo.com; amqureshi@bzu.edu.pk

R. Hussain · M. Q. Fatmi · H. Bokhari
Department of Biosciences, COMSATS Institute of Information
Technology, Chak Shahzad, Islamabad, Pakistan

A. Rauf
Department of Chemistry, The Islamia University, Bahawalpur,
Pakistan

M. Oelgemöller
James Cook University, School of Pharmacy and Molecular
Sciences, Townsville, QLD 4811, Australia



Scheme 1 X = O, R = COCH₃, (2) X = O, R = NH-C=S-NH₂, (3) X = O, R = NH-C=ONHPh, (4) X = S, R = NH-C=ONHPh, (5) X = S, R = NH-C=SNHPh, (6) X = S, R = NH-C=SNH-p-F-Ph, (7) X = S, R = NH-C=SNH-p-Cl-Ph, (8) X = O, R = NH-

C=SNH-o-CH₃, p-Cl-Ph, (9) X = S, R = NH-C=SNH-p-Br-Ph, (10) X = O, R = NH-C=SNH-m-CF₃-Ph, (11) X = S, R = NH-C=SNH-p-CF₃-Ph, (12) X = S, R = NH-C=SNH-p-OCH₃-Ph, (13) X = O, R = NH-C=SNH-p-CN-Ph

anionic site (Hucho *et al.*, 1991; Quinn, 1987). AChE functions in rapid hydrolysis of acetylcholine at cholinergic synapses (Allderdice *et al.*, 1991), while BChE is important for detoxification and hydrolysis of ester-containing drugs, as well as, scavenging of cholinesterase inhibitors, prior reaching their synaptic targets. Cholinesterase inhibitors are important for treatment of various diseases like organophosphate poisoning (Sussman *et al.*, 1991), myasthenia gravis, glaucoma, and promisingly Alzheimer disease (AD) (Gilman *et al.*, 1990; Hallak and Giacobini, 1989).

In present study, anticholinesterase activity of 13 barbiturates/thiobarbiturates was evaluated. All synthesized compounds were docked into active sites of AChE and BChE and binding models were constructed.

Results and discussion

Chemistry

For synthesis, to a refluxing solution of thio/barbituric acid and triethylorthoformate in 2-butanol was added respective amine (Scheme 1). Precipitates formed were collected and washed with hot ethanol offering pure products in excellent yields (88–94 %) (Rauf *et al.*, 2012). Structures of the synthesized compounds were deduced by analytical and spectroscopic (¹H NMR, ¹³C NMR, and EIMS) data. Satisfactory elemental analyses (± 0.4 % of calculated values) were obtained for all the compounds. In EI mass spectra, all the compounds showed molecular ions of different intensity, which confirmed their molecular weights. Few of the compounds did not show the molecular ion peaks in their spectra. However, the fragments corresponding to thiosemicarbazone moiety, formed by the cleavage of N–N and NH–CS bonds confirmed their structures.

Antibacterial activity (in vitro)

The compounds were subjected for bacterial activity against three Gram-negative (*Escherichia coli*, *Pseudomonas aeruginosa*, and *Salmonella typhi*) and one Gram-positive (*Staphylococcus aureus*) bacterial strains at 1 mg/mL in

DMSO. Of these, only **1** and **2** displayed moderate activity against three strains, i.e., *E. coli*, *P. aeruginosa*, and *S. aureus* (Tables 1, 2).

In vitro cholinesterase activity

Bioassay results for enzyme inhibition are represented in Fig. 1 and Table 3. Nineteen compounds showed reportable IC₅₀ value against AChE of which **10** appeared as a most potent inhibitor with IC₅₀ value 40.78 μ M at 0.5 mM. On the whole all such compounds are mostly, excellent BChE inhibitors. Compound **4** showed maximum inhibition, thus acts as the most potent inhibitor with IC₅₀ value of 3.31 \pm 0.08 μ M at 0.125 mM followed by **11** and **8** with IC₅₀ values of 8.11 and 8.81 μ M at 0.5 mM, respectively. Structure–activity relationship studies revealed that electrostatic effects of the substituents play an important role in the enzyme inhibitory potential of the synthetic compounds.

Docking

Biological assay and docking analysis

In order to rationalize ligand–protein interaction for establishing SAR, molecular docking studies of all synthesized barbiturate or thiobarbiturates were performed against AChE and BChE. Compound **10** indicated a better docking score, –10.20 kcal/mol, against AChE as compared to the reference inhibitor, eserine, –7.10 kcal/mol. Likewise, compounds **4**, **11**, and **8** exhibited better binding energy values of –9.30, –9.50, and –8.50 kcal/mol, respectively, against BChE as compared to that of the reference inhibitor, eserine, i.e., –7.50 kcal/mol.

Binding model of compound **10** in the active site of AChE is depicted in Fig. 2a, which clearly demonstrates that both amino and amido groups of the ligand form H-bonds with the carboxylic acid group of Tyr124 (bond distance 3.26 Å) and Tyr337 (bond distance 3.26 Å). Another H-bond with comparatively short distance is formed by the nitrogen of pyrimidinetrione ring with the oxygen of Ser203 (bond distance 2.97 Å). Compound **10**

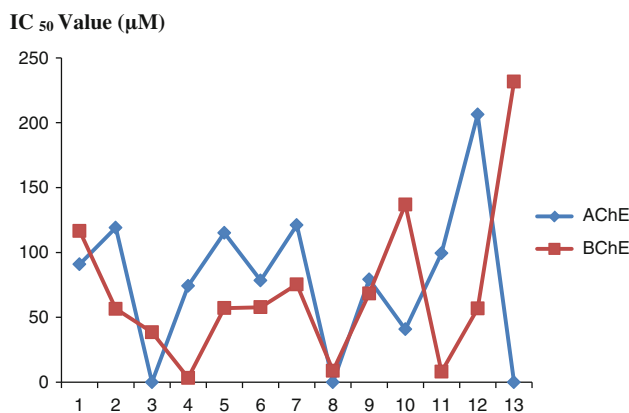
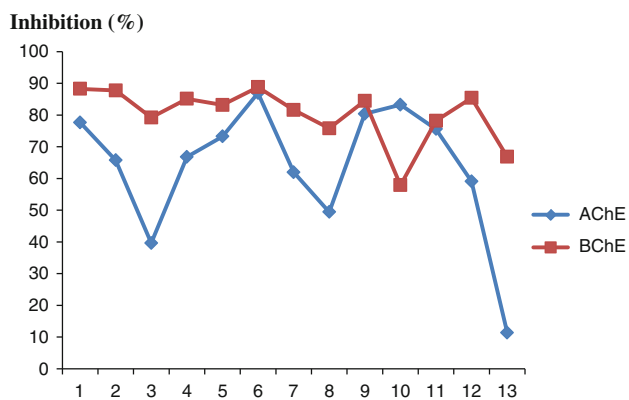
Table 1 Antibacterial activity (1)–(13)

Compound (1 mg/mL)	Zone of inhibition in “mm”						
	<i>E.coli</i>			<i>P. aeruginosa</i>	<i>S. typhi</i>	<i>V. cholera</i>	<i>S. aureus</i>
	<i>DH5α</i>	<i>DG2</i>	<i>5604</i>				
1	15	–	–	18	–	–	18
7	14	–	–	–	–	–	15
Chloramphenicol	25	–	–	25	–	–	25

– No activity

Table 2 Minimum inhibitory concentration of the active compounds

Compound	MIC (μ g/mL)		
	<i>E. coli</i> (<i>DH5 α</i>)	<i>P. aeruginosa</i>	<i>S. aureus</i>
1	100	200	100
7	200	400	100
Chloramphenicol	1.56	1.56	<0.78

**Fig. 1** Graphical representation of compounds (1–13) activity in terms of % inhibition (a) and IC_{50} values (b), where series1: *Acetyl cholinesterase*; and series2: *Butyryl cholinesterase*

also exhibits π – π interactions by each Trp286 and Tyr341 (Fig. 2a). Most of the residues such as Ala204, Trp86, Phe297, and Phe338 are involved in van der Waal

interactions with pyrimidinetrione ring of the inhibitor, which clearly demonstrate that a significant contribution for ligand binding has come through van der Waal interactions. The order of activity among 13 compounds as determined experimentally is **10** > **4** > **6** > **9** > **1** > **11** > **5** > **13** > **2** > **7**. The binding models of these compounds with AChE indicate Ser203, Tyr124, Tyr337, Tyr341, Trp86, Trp286, Phe297, Phe338, Glu202, and His447 as common residues, involved in ligand interactions, and therefore, indicate their importance in ligand binding as well as in possible catalytic activities. These residues may also play a vital role in lead optimization, and thereby, aid in improving the ligand affinity with the protein. Other residues that interact with receptor site but not present commonly are Ala204, Phe295, Asp74, Tyr72, and Gly122 (Table 4).

Binding models of **4**, **11**, and **8** in the active site of BChE are depicted in Fig. 2b–d, respectively. Compound **4** exhibits H-bond with the active site residue, Gly117, of BChE through the oxygen of acetamide group with a distance of 3.39 Å. A comparatively weak H-bond can also be observed between the nitrogen of acetamide group and the carboxylic acid moiety of Ser198 (bond distance 4.00 Å). Both nitrogen atoms of thiopyrimidinedione ring are involved in H-bonding with the same oxygen of Gly115 (bond distance 3.15 Å) and Thr120 (bond distance 3.39 Å). Compound **4** also contribute in binding through π – π interaction with Trp231, and interact electrostatically with Glu197 and Ala199. Whereas, residues Tyr114, Ile69, Leu125, Phe329, Phe398, and Trp82 are involved in van der Waal interactions with thiopyrimidinedione ring of the inhibitor (Fig. 2b). The nitrogen of hydrazine group in compound **11** displays a moderately strong H-bond with the hydroxyl group of Tyr332 (bond distance 2.87 Å). Furthermore, both nitrogen atoms of thiopyrimidinedione ring show H-bond interactions with hydroxyl groups of Asn83 (bond distance 3.02 Å) and Thr120 (bond distance 2.93 Å). A π – π interaction can also be observed in compound **11**, where Trp82 of BChE is involved with trifluorobenzene ring of the ligand. Residues His438 and Tyr128 are interacting electrostatically with the compound **11**,

Table 3 Acetyl and butyryl cholinesterase inhibition with their IC₅₀ values

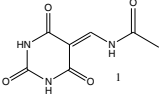
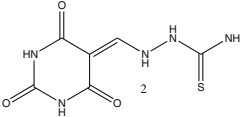
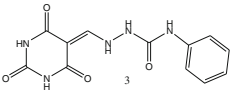
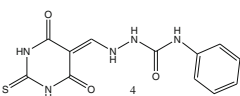
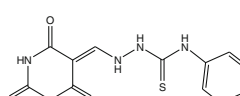
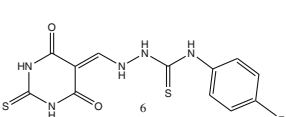
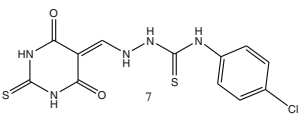
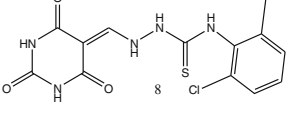
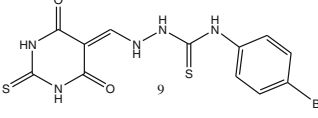
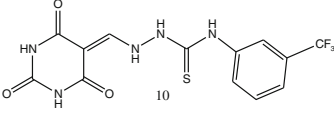
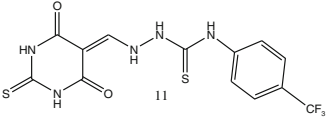
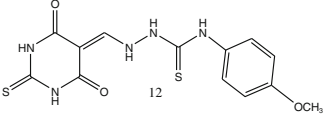
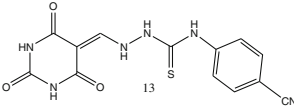
Compound structure and code	Inhibition %		IC ₅₀ (μmol)		Binding energy (kcal/mol)	
	AChE	BChE	AChE	BChE	AChE	BChE
	77.65 ± 0.72 ^a	88.26 ± 0.71 ^a	90.91 ± 0.33 ^a	116.61 ± 0.24 ^a	-7.90	-7.10
	65.75 ± 0.71 ^a	87.52 ± 0.92 ^a	119.11 ± 0.24 ^a	56.51 ± 0.18 ^a	-7.60	-6.40
	39.61 ± 0.12 ^b	79.21 ± 0.11 ^b	NIL ^b	38.51 ± 0.01 ^b	-10.20	-9.60
	66.80 ± 0.28 ^b	85.12 ± 0.06 ^b	74.21 ± 0.01 ^b	3.31 ± 0.08 ^b	-9.40	-9.30
	73.23 ± 0.44 ^a	83.18 ± 0.14 ^a	115.11 ± 0.17 ^a	57.11 ± 0.36 ^a	-8.80	-8.50
	86.93 ± 0.64 ^a	88.82 ± 0.24 ^a	78.41 ± 0.25 ^a	57.81 ± 0.14 ^a	-8.80	-8.60
	61.96 ± 0.14 ^a	81.61 ± 0.42 ^a	121.11 ± 0.01 ^a	75.41 ± 0.28 ^a	-9.40	-8.20
	49.41 ± 0.56	75.79 ± 0.64	NIL	8.81 ± 0.02	-9.90	-8.50
	80.39 ± 0.17 ^a	84.47 ± 0.74 ^a	79.21 ± 0.08 ^a	68.41 ± 0.21 ^a	-9.40	-8.10
	83.26 ± 0.35	75.88 ± 0.63	40.78 ± 0.35	136.91 ± 0.08	-10.20	-9.30
	75.56 ± 0.11 ^a	78.19 ± 0.45 ^a	99.41 ± 0.31 ^a	8.11 ± 0.24 ^a	-9.90	-9.50
	59.08 ± 0.63 ^a	85.41 ± 0.44 ^a	206.31 ± 0.06 ^a	56.81 ± 0.02 ^a	-8.80	-8.10

Table 3 continued

Compound structure and code	Inhibition %		IC ₅₀ (μmol)		Binding energy (kcal/mol)	
	AChE	BChE	AChE	BChE	AChE	BChE
	11.37 ± 0.62 ^a	66.82 ± 0.28 ^a	NIL ^a	231.61 ± 0.55 ^a	-10.10	-8.80
^R Eserine	92.54 ^a	92.54 ^a	0.04 ± 0.001 ^a	0.85 ± 0.001 ^a	-7.10	-7.50

Methanol was used as solvent and concentration of all the samples was 0.5 mM

R reference inhibitor of the enzyme

^a Stands for 0.25 mM concentration of sample and ^b for 0.125 mM

whereas, Pro84 and Gly121 are involved in van der Waal interactions with thiopyrimidinedione ring of the inhibitor (Fig. 2c). Compound **8** binds to BChE through nitrogen as well as oxygen atoms of pyrimidinetrione ring, and forms H-bonds with hydroxyl group of Pro285 (bond distance 3.38 Å) and amino group of Gly117 (bond distance 2.88 Å), respectively. One comparatively weaker H-bond between the nitrogen of hydrazine group of ligand and the hydroxyl group of Ser198 (bond distance 4.24 Å) can also be observed. Compound **8** is further involved in π - π interaction with Trp82 through its chloromethyl benzene ring. BChE residues Glu197, His438, Tyr332, and Tyr440 are interacting electrostatically with the ligand, whereas Ala199, Phe329, and Phe398 are involved in van der Waal interactions with pyrimidinetrione ring and Trp430 with chloromethyl benzene ring of the inhibitor (Fig. 2d). On the basis of experimental IC₅₀ values, the activity of compounds is sorted as **4** > **11** > **8** > **3** > **12** > **5** > **6** > **9** > **2**. With few exceptions, this trend in activity gets support from docking studies as well (Table 3). Common residues which are involved in complex interaction are: Trp82, His438, Trp231, Ala199, Phe398, Tyr332, Tyr128, Pro285, and Ser198. Other residues that interact with the receptor site but not present commonly are Gly115, Gly117, Asn83, Thr120, Glu197, Tyr430, and Tyr440 (Table 5). These common interacting residues in BChE highlight the role of these residues in ligand binding as well as in their catalytic activities, which can further be explored by mutational dynamics simulation studies, and verified by experiments.

Conclusions

In conclusion, several barbiturates and thiobarbiturates were synthesized and characterized through ¹H NMR, ¹³C NMR, EIMS, and elemental analysis. Antibacterial assay showed that two of the compounds were found to be moderately active against three different bacterial strains.

Results from in vitro and docking studies revealed similar outcomes, regarding inhibitory activity on AChE, and BChE. Present work will add in existing knowledge about inhibition mechanism of AChEI and BChEI, such as, a better understanding of interaction of active sites of enzyme with barbiturates or thiobarbiturates.

Experimental

Melting points were taken on a Fisher-Johns melting point apparatus and are uncorrected. Elemental analyses were performed on a Leco CHNS-9320 elemental analyzer. ¹H and ¹³C NMR spectra were recorded in DMSO-*d*₆ on Bruker (Rhenistetten-Forchheim, Germany) NMR spectrometer at 300 and 75.4 MHz respectively. The electron impact mass spectra (EIMS) were determined with a Finnigan MAT-312 and a JEOL MS Route mass spectrometer.

General procedure for the preparation of compounds (1)–(13)

To a hot stirred solution of thio/barbituric acid (2.00 mmol) and ethylorthoformate (2.02 mmol) in 2-butanol (10 mL) was added the respective amine (2.00 mmol). Then the reaction mixture was refluxed till the completion of the reaction (for ≈ 3 h). The precipitates formed were collected by suction filtration. Washing with hot ethanol afforded pure products in good to excellent yield.

N-[(2,4,6-trioxotetrahydropyrimidin-5(2H)-ylidene)methyl]acetamide (**1**) Yield 88 % as yellow solid; m.p. 240 °C; ¹H NMR (300 MHz, DMSO-*d*₆, δ , ppm): 2.83 (3H, s, CH₃), 4.51 (1H, s, NHC(=O)CH₃), 7.82 (1H, s, =CH), 10.51 (2H, s, NHBA); ¹³C NMR (300 MHz, DMSO-*d*₆, δ , ppm): 170 (C=O amide), 150 (C=O amide), 145 (CH ethylene), 95 (C ethylene), 25 (CH₃); EIMS (70 eV) *m/z* (%): ([M+],

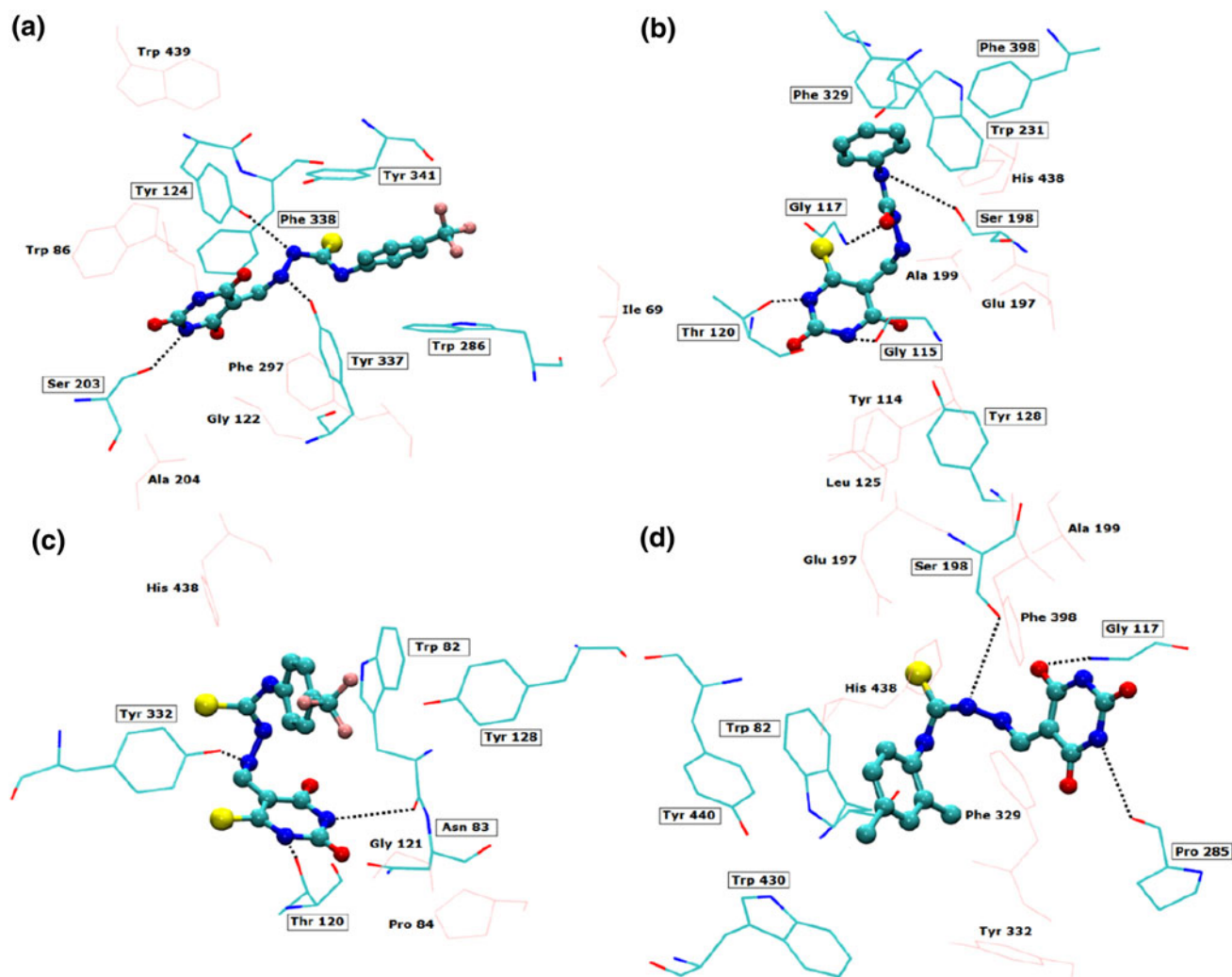


Fig. 2 Complex binding models of (a) **32** with AChE and (b–d) **10**, **34**, and **24**, respectively, with BChE. Protons are omitted for clarity

197 (100)), 183 (61), 155 (48), 140 (22), 127 (6), 77 (11), 63 (14), 50 (8), 44 (17); (Found: C, 42.66; H, 3.53; N, 21.33 %. Calc. For $C_7H_7N_3O_4$: C, 42.64; H, 3.55; N, 21.32 %).

2-[(2,4,6-trioxotetrahydropyrimidin-5(2H)-ylidene)methyl]hydrazinecarbothioamide (2) Yield 90 % as orange yellow solid; m.p. 210 °C; 1H NMR (300 MHz, DMSO- d_6 , δ , ppm): 7.81 (3H, s, NH_2), 9.14 (1H, s, =CH), 10.12 (2H, s, NH NH), 11.11 (2H, s, $NHBA$); ^{13}C NMR (300 MHz, DMSO- d_6 , δ , ppm) 181(C=S thiamide), 164 (C=O amide), 163 (C=O amide), 151 (C=O amide), 116 (CH ethylene), 96 (C ethylene); EIMS (70 eV) m/z (%): ([M+], 229 (100)), 186 (61), 158 (48), 144 (22), 136 (22), 127 (6), 115 (20), 101 (5), 89 (25), 77 (11), 63 (14), 50 (8), 44 (17); (Found: C, 31.45; H, 3.08; N, 30.55; S, 13.96 %. Calc. For $C_6H_7N_5O_3S$: C, 31.44; H, 3.06; N, 30.57; S, 13.97 %).

N-phenyl-2-[(2,4,6-trioxotetrahydropyrimidin-5(2H)-ylidene)methyl]hydrazinecarboxamide (3) Yield 90 % as yellow solid; m.p. 220 °C; 1H NMR (300 MHz, DMSO- d_6 , δ , ppm): 5.65 (2H, s, $NHAr$), 7.04 (1H, m, ArH), 7.26 (2H, m, ArH), 7.48 (1H, m, ArH), 7.96 (1H, d, J 9, ArH), 8.77 (1H, s, =CH), 10.50 (2H, s, NH NH), 11.00 (2H, s, $NHBA$); ^{13}C NMR (300 MHz, DMSO- d_6 , δ , ppm), 158 (C=O amide), 154 (C=O amide), 150 (CH ethylene), 139 (C benzene), 128(CH benzene), 121(CH benzene), 118 (CH benzene), 89 (C ethylene); EIMS (70 eV) m/z (%): ([M+], 289 (2)), 261 (5), 231 (3), 199 (3), 170 (22), 154 (15), 128 (5), 119 (100), 93 (94), 77 (20), 66 (34), 51 (8), 43 (14); (Found: C, 50.01; H, 3.45; N, 24.29, O %. Calc. For $C_{12}H_{10}N_5O_4$: C, 50.00; H, 3.47; N, 24.31 %).

2-[(4,6-dioxo-2-thioxotetrahydropyrimidin-5(2H)-ylidene)methyl]-N-phenylhydrazine carboxamide (4) Yield 92 % as yellow solid; m.p. 274 (dec.) °C; 1H NMR (300 MHz,

Table 4 Interactions of AChE against selected top 10 active inhibitors based on IC₅₀ value

CN	H-bonding		π - π Interactions	Electrostatic interactions	VDW
	Interacting residues	Distance (Å)			
10	Ser203:OH...N:C ₄ H ₂ N ₂ O ₃	2.97	Trp286 with C ₆ H ₄ -CF ₃		*Ala204 with C ₄ H ₂ N ₂ O ₃
	Tyr337:OH...N:NHNH ₂	3.26	Tyr341 with C ₆ H ₄ -CF ₃		Trp86 with C ₄ H ₂ N ₂ O ₃
	Tyr124:OH...N:NHNH ₂	3.26			Phe338 with C ₄ H ₂ N ₂ O ₃ ring Phe297 C ₄ H ₂ N ₂ O ₃ Gly122 C ₄ H ₂ N ₂ O ₃
4	Gly120:b OH...N:C ₄ H ₂ N ₂ O ₂ S	3.76	Tyr341 with C ₆ H ₅ -NH	Glu202 with C ₆ H ₅ -NH	Trp86 with C ₄ H ₂ N ₂ O ₂ S
	Ser203:OH...N:C ₄ H ₂ N ₂ O ₂ S	3.18		His447 with NHNH ₂	Ala204 with C ₄ H ₂ N ₂ O ₂ S
	Tyr337:OH...N:NHNH ₂	2.80			Trp286 with C ₆ H ₅ -NH
	Tyr124:OH...N:NHNH ₂	2.77			Phe295 with C ₆ H ₅ -NH Phe297 with C ₆ H ₅ -NH Phe338 with C ₆ H ₅ -NH
6	Tyr124:OH...N:NHNH ₂	3.34	Tyr341 with C ₆ H ₄ F	Glu202 with C ₄ H ₂ N ₂ O ₂ S	Trp86 with C ₄ H ₂ N ₂ O ₂ S
	Gly120:b OH...N:C ₄ H ₂ N ₂ O ₂ S	3.54		His447 with NHNH ₂	Ala204 with C ₄ H ₂ N ₂ O ₂ S
	Tyr337:OH...N:NHNH ₂	2.99			Phe297 with C ₆ H ₄ F Phe338 with C ₆ H ₄ F Phe295 with C ₆ H ₄ F Trp286 with C ₆ H ₄ F
9	Tyr124:OH...N:NHNH ₂	2.72	Tyr341 with C ₆ H ₄ Br	Glu202 with C ₄ H ₂ N ₂ O ₂ S	Phe297 with NHNH ₂
	Ser203:OH...N:C ₄ H ₂ N ₂ O ₂ S	3.16	Trp286 with C ₆ H ₄ Br	His447 with C ₄ H ₂ N ₂ O ₂ S	Phe295 C ₄ H ₂ N ₂ O ₂ S
	Tyr337:OH...N:NHNH ₂	3.15			Phe338 with C ₄ H ₂ N ₂ O ₂ S & NHNH ₂ Tyr72 with C ₆ H ₄ Br Trp86 with C ₄ H ₂ N ₂ O ₂ S
1	Gly126:b NH...O:CONH	3.32		Glu202 with C ₄ H ₂ N ₂ O ₃	Trp86 with C ₄ H ₂ N ₂ O ₃
	Tyr337:OH...N:C ₄ H ₂ N ₂ O ₃	3.34		His447 with C ₄ H ₂ N ₂ O ₃	Trp439 with C ₄ H ₂ N ₂ O ₃ (weak)
	His447:b OH...N:C ₄ H ₂ N ₂ O ₃	3.36			Phe338 with C ₄ H ₂ N ₂ O ₃
11	Tyr337:OH...N:NHNH ₂	3.19	Tyr341 with C ₆ H ₄ -CF ₃	Glu202 with C ₄ H ₂ N ₂ O ₂ S	Phe297 with NHNH ₂
	Ser203:OH...N:C ₄ H ₂ N ₂ O ₂ S	3.14	Trp286 with C ₆ H ₄ -CF ₃	His447 with C ₄ H ₂ N ₂ O ₂ S	Phe295 C ₄ H ₂ N ₂ O ₂ S
	Tyr124:OH...N:NHNH ₂	3.19			Phe338 with C ₄ H ₂ N ₂ O ₂ S & NHNH ₂ Tyr72 with C ₆ H ₄ -CF ₃ Trp86 with C ₄ H ₂ N ₂ O ₂ S
5	Tyr124:OH...N:NHNH ₂	2.81, 3.26	Trp286 with C ₆ H ₅ -NH	ASP74 with C ₆ H ₅ -NH	Trp86 with C ₄ H ₂ N ₂ O ₂ S
	Ser203:OH...N:C ₄ H ₂ N ₂ O ₂ S	3.03	Tyr341 with C ₆ H ₅ -NH	Glu202 with C ₄ H ₂ N ₂ O ₂ S His447 with C ₄ H ₂ N ₂ O ₂ S	Ala204 with C ₄ H ₂ N ₂ O ₂ S Phe297 with NHNH ₂ Tyr72 with C ₆ H ₅ -NH Phe338 with NHNH ₂
13	Ser203:OH...N:C ₄ H ₂ N ₂ O ₃	3.00	Tyr341 with C ₆ H ₄ -CN	ASP74 with C ₆ H ₄ -CN	Phe338 with NHNH ₂
	Tyr337:OH...N:NHNH ₂	3.32	Trp286 with C ₆ H ₄ -CN	Glu202 with C ₄ H ₂ N ₂ O ₃	Phe297 with C ₄ H ₂ N ₂ O ₃
	Tyr124:OH...N:NHNH ₂	2.80		His447 with C ₄ H ₂ N ₂ O ₃	Tyr72 with C ₆ H ₄ -CN
2	Tyr337:OH...N:NHNH ₂	2.96		ASP74 with CSNH	Trp86 with NHNH ₂
	Tyr341:OH...N:CSNH	3.27		Glu202 with C ₄ H ₂ N ₂ O ₃	Ala204 with C ₄ H ₂ N ₂ O ₃
	Asp74:O-N:CSNH	3.08		His447 with C ₄ H ₂ N ₂ O ₃	Phe297 with C ₄ H ₂ N ₂ O ₃
	Ser203:OH...N:C ₄ H ₂ N ₂ O ₃	2.82			Phe295 with C ₄ H ₂ N ₂ O ₃
7	Ser203:OH...N:C ₄ H ₂ N ₂ O ₂ S	3.14	Tyr341 with C ₆ H ₄ Cl	ASP74 with C ₆ H ₄ Cl	Trp86 with C ₄ H ₂ N ₂ O ₂ S
	Tyr337:OH...N:NHNH ₂	3.23	Trp286 with C ₆ H ₄ Cl	Glu202 with C ₄ H ₂ N ₂ O ₂ S	Ala204 with C ₄ H ₂ N ₂ O ₂ S
	Tyr124:OH...N:NHNH ₂	2.71		His447 with C ₄ H ₂ N ₂ O ₂ S	Phe297 with NHNH ₂ Phe295 with C ₄ H ₂ N ₂ O ₂ S

Table 5 Interactions of BChE selected top 9 active inhibitors based on IC₅₀ value

CN	H-bonding		π - π Interactions	Electrostatic interactions	VDW
	Interacting residues	Distance (Å)			
4	Thr120:O...N:C ₄ H ₂ N ₂ O ₂ S	3.39		Glu197 with NHNH ₂	Tyr114 with C ₄ H ₂ N ₂ O ₂ S
	Gly117:b NH...O:CONH	3.39		Ala199 with CO	Ile69 with C ₄ H ₂ N ₂ O ₂ S
	Ser198:OH...N:CONH	4			Leu125 with C ₄ H ₂ N ₂ O ₂ S
	Gly115:b OH...N:NHNH ₂	3.15			Phe398 with C ₆ H ₅ -NH Trp231 with C ₆ H ₅ -NH Phe329 with C ₆ H ₅ -NH Trp82 with C ₄ H ₂ N ₂ O ₂ S
11	Asn83:b OH...N:C ₄ H ₂ N ₂ O ₂ S	3.02	Trp82 with C ₆ H ₄ -CF ₃	His438 with CONH	Pro84 with C ₄ H ₂ N ₂ O ₂ S
	Tyr332:OH...N:NHNH ₂	2.87		Tyr128 with C ₆ H ₄ -CF ₃	Gly121 with C ₄ H ₂ N ₂ O ₂ S
	Thr120:O...N:C ₄ H ₂ N ₂ O ₂ S	2.93			
8	Pro285:O...N:C ₄ H ₂ N ₂ O ₃	3.38	Trp82 with C ₇ H ₆ Cl	Glu197 with CSNH	Phe329 with C ₄ H ₂ N ₂ O ₃ and NHNH ₂
	Gly117:N...O:C ₄ H ₂ N ₂ O ₃	2.881		His438 with NHNH ₂	Phe398 with C ₄ H ₂ N ₂ O ₃
	Ser198:OH...N:NHNH ₂	4.24		Tyr440 with C ₇ H ₆ Cl	Ala199 with C ₄ H ₂ N ₂ O ₃
3	Ser198:OH...O:CO	3.03		Tyr332 with C ₇ H ₆ Cl	Trp430 with C ₇ H ₆ Cl
	His438:OH...N:C ₄ H ₂ N ₂ O ₃	3.22		His438 with C ₄ H ₂ N ₂ O ₃	Trp82 with C ₄ H ₂ N ₂ O ₃
	Trp82:NH...N:C ₄ H ₂ N ₂ O ₃	3.62		Ala199 with CO	Tyr440 with C ₄ H ₂ N ₂ O ₃ Trp231 with C ₆ H ₅ -NH Gly439 with C ₄ H ₂ N ₂ O ₃ Gly117 with NHNH ₂ Gly115 with NHNH ₂ Phe329 with C ₆ H ₅ -NH Phe398 with C ₆ H ₅ -NH
12	Ser287:b OH...O:C ₄ H ₂ N ₂ O ₂ S	3.46	Trp82 with C ₆ H ₄ -OCH ₃	Tyr332 with C ₆ H ₄ -OCH ₃	Trp231 with C ₄ H ₂ N ₂ O ₂ S
	Ser287:OH...O:C ₄ H ₂ N ₂ O ₂ S	2.77		Glu197 with NHNH ₂	Trp430 with C ₆ H ₄ -OCH ₃
	His438:N...N:NHNH ₂	3.21			Tyr128 with CSNH Gly78 with C ₆ H ₄ -OCH ₃ Gly439 with C ₆ H ₄ -OCH ₃ Ala199 with C ₄ H ₂ N ₂ O ₂ S Pro285 with C ₄ H ₂ N ₂ O ₂ S
5	Pro285:b OH...N:CSNH	3.27		Glu197 with C ₄ H ₂ N ₂ O ₂ S	Phe398 with C ₆ H ₅ -NH
	His438:NH...O:CSNH	2.99	-	Ala199 with C ₆ H ₅ -NH	Phe329 with C ₆ H ₅ -NH Phe398 with C ₆ H ₅ -NH Trp231 with C ₆ H ₅ -NH Trp82 with C ₄ H ₂ N ₂ O ₂ S
	Tyr128:OH...O:C ₄ H ₂ N ₂ O ₂ S	2.78			
6	Pro285:b OH...N:CSNH	3.24		His438 with C ₄ H ₂ N ₂ O ₂ S	Trp231 with C ₆ H ₄ F
	Glu197:O...N:C ₄ H ₂ N ₂ O ₂ S	3.31		Tyr128 with C ₄ H ₂ N ₂ O ₂ S	Phe329 with C ₆ H ₄ F
	Gly115:b N...O:C ₄ H ₂ N ₂ O ₂ S	3.68		Glu197 with C ₄ H ₂ N ₂ O ₂ S	Phe398 with C ₆ H ₄ F
9	Asn83:b OH...N:C ₄ H ₂ N ₂ O ₂ S	2.92	Trp82 with C ₆ H ₄ Br	Ala199 with C ₆ H ₄ F	His438 with C ₆ H ₄ Br
	Asp70:O...N:NHNH ₂	3.04	Glu197 with C ₆ H ₄ Br		Phe329 with CSNH
	Tyr332:OH...N:NHNH ₂	2.87			
2	Ser198:OH...N:C ₄ H ₂ N ₂ O ₃	3.18	Trp82 with C ₆ H ₄ Br		
	Trp231:N...O:C ₄ H ₂ N ₂ O ₃	3.29			
	His438:NH...O:C ₄ H ₂ N ₂ O ₃	3.01			

DMSO- d_6 , δ , ppm): 4.59 (1H, s, NHAr), 7.00 (1H, m, ArH), 7.20 (2H, m, ArH), 7.40 (2H, m, ArH), 8.77 (1H, s, =CH), 9.34 (2H, s, NHNH), 12.01 (2H, s, NHBA); ^{13}C NMR (300 MHz, DMSO- d_6 , δ , ppm) 197 (C=S thiamide), 177 (C=O amide), 161 (C=O amide), 157 (CH ethylene), 155 (C benzene), 128 (CH benzene), 122 (CH benzene), 118 (CH benzene), 91 (C ethylene); EIMS (70 eV) m/z (%): ([M+], 305 (3)), 274 (2), 247 (5), 199 (3), 177 (35), 151 (51), 119 (100), 93 (89), 77 (54), 64 (48), 51 (16), 44 (51); (Found: C, 47.38; H, 3.27; N, 23.04; S, 10.55 %. Calc. For $\text{C}_{12}\text{H}_{10}\text{N}_5\text{O}_3\text{S}$: C, 47.37; H, 3.29; N, 23.03; S, 10.53 %).

2-[(4,6-dioxo-2-thioxotetrahydropyrimidin-5(2H)-ylidene)methyl]-N-phenylhydrazine carbothioamide (**5**) Yield 93 % as yellow solid; m.p. 180 (dec.) °C; ^1H NMR (300 MHz, DMSO- d_6 , δ , ppm): 4.28 (1H, s, NHAr), 6.97 (1H, m, ArH), 7.01 (1H, m, ArH), 7.13 (1H, t, J 9,15, ArH), 7.33 (1H, t, J 9,15, ArH), 7.55 (1H, d, J 6, ArH), 8.03 (1H, s, =CH), 9.76 (2H, s, NHNH), 11.41 (1H, s, NHBA), 11.76 (1H, s, NHBA); ^{13}C NMR (300 MHz, DMSO- d_6 , δ , ppm) 179 (C=S thiamide), 167 (C=O amide), 160 (C=O amide), 153 (CH ethylene), 139 (C benzene), 129 (CH benzene), 128 (CH benzene), 124 (CH benzene), 113 (CH benzene), 99 (C ethylene); EIMS (70 eV) m/z (%): ([M+], 321 (3)), 268 (27), 247 (75), 185 (2), 167 (20), 143 (5), 135 (74), 116 (54), 104 (12), 93 (33), 77 (71), 69 (36), 59 (21), 43 (45); (Found: C, 44.87; H, 3.42; N, 21.80; S, 19.93 %. Calc. For $\text{C}_{12}\text{H}_{11}\text{N}_5\text{O}_2\text{S}_2$: C, 44.86; H, 3.43; N, 21.81; S, 19.94 %).

2-[(4,6-dioxo-2-thioxotetrahydropyrimidin-5(2H)-ylidene)methyl]-N-(4-fluorophenyl) hydrazinecarbothioamide (**6**) Yield 92 % as yellow solid; m.p. 218 °C; ^1H NMR (300 MHz, DMSO- d_6 , δ , ppm): 5.00 (1H, s, NHAr), 7.49 (2H, m, ArH), 7.17 (2H, m, ArH), 8.13 (1H, s, =CH), 9.91 (2H, s, NHNH), 11.99 (2H, s, NHBA); ^{13}C NMR (300 MHz, DMSO- d_6 , δ , ppm) 177 (C=S thiamide), 161 (C=O amide), 153 (CF benzene), 135 (CH ethylene), 128 (C benzene), 125 (CH benzene), 115 (CH benzene), 114 (CH benzene), 90 (C ethylene); EIMS (70 eV) m/z (%): 304 (13), 265 (76), 227 (14), 207 (4), 195 (15), 186 (81), 171 (24), 153 (87), 144 (49), 126 (67), 116 (18), 111 (100), 98 (2), 95 (37), 84 (42), 69 (17), 59 (24), 43 (13); (Found: C, 42.49; H, 2.94; N, 20.66; S, 18.89 %. Calc. For $\text{C}_{12}\text{H}_{10}\text{N}_5\text{O}_2\text{S}_2\text{F}$: C, 42.48; H, 2.95; N, 20.65; S, 18.88 %).

N-(4-chlorophenyl)-2-[(4,6-dioxo-2-thioxotetrahydropyrimidin-5(2H)-ylidene)methyl] hydrazinecarbothioamide (**7**) Yield 90 % as yellow solid; m.p. 220 °C; ^1H NMR (300 MHz, DMSO- d_6 , δ , ppm): 4.38 (1H, s, NHAr), 7.37 (2H, d, J 9, ArH), 7.58 (2H, d, J 9, ArH), 8.04 (1H, s, =CH), 9.84 (2H, s, NHNH), 11.39 (1H, s, NHBA), 11.76 (1H, s, NHBA); ^{13}C NMR (300 MHz, DMSO- d_6 , δ , ppm)

197 (C=S thiamide), 167 (C=O amide), 163 (C=O amide), 151 (CCl benzene), 148 (CH ethylene), 138 (C benzene), 127 (CH benzene), 118 (CH benzene); EIMS (70 eV) m/z (%): ([M+], 355 (2)), 339(3), 304 (4), 288 (3), 272 (3), 242(2), 211 (9), 201(11), 184 (13), 169(100), 141 (5), 111 (67), 101 (6), 90 (16), 75 (32), 65 (14), 44 (47); (Found: C, 40.50; H, 2.82; N, 12.69; S, 18.01 %. Calc. For $\text{C}_{12}\text{H}_{10}\text{N}_5\text{O}_2\text{S}_2\text{Cl}$: C, 40.51; H, 2.81; N, 12.69; S, 18.00 %).

N-(2-chloro-6-methylphenyl)-2-[(2,4,6-trioxotetrahydropyrimidin-5(2H)-ylidene)methyl] hydrazinecarbothioamide (**8**) Yield 91 % as yellow solid; m.p. 310 (dec.) °C; ^1H NMR (300 MHz, DMSO- d_6 , δ , ppm): 3.86 (3H, s, CH₃), 4.38 (1H, s, NHAr), 7.37 (1H, m, ArH), 7.58 (2H, m, ArH), 8.50 (1H, s, =CH), 9.89 (2H, s, NHNH), 11.03 (2H, s, NHBA); ^{13}C NMR (300 MHz, DMSO- d_6 , δ , ppm) 197 (C=S thiamide), 168 (C=O amide), 163 (C=O amide), 151 (CCl benzene), 137 (CH ethylene), 126 (C benzene), 117 (CH benzene), 91 (CH benzene), 87 (C ethylene), 18 (CH₃); EIMS (70 eV) m/z (%): ([M+], 353 (2)), 339 (3), 304 (78), 288 (3), 279 (46), 229 (2), 211 (9), 201 (11), 184 (13), 169(100), 141 (5), 128 (67), 106 (6), 85 (16), 69 (32), 51 (14), 42 (47); (Found: C, 44.02; H, 3.68; N, 19.74; S, 9.02 %. Calc. For $\text{C}_{13}\text{H}_{13}\text{N}_5\text{O}_3\text{SCl}$: C, 44.01; H, 3.67; N, 19.75; S, 9.03 %).

N-(4-bromophenyl)-2-[(4,6-dioxo-2-thioxotetrahydropyrimidin-5(2H)-ylidene)methyl] hydrazinecarbothioamide (**9**) Yield 89 % as yellowish orange solid; m.p. 220 (dec.) °C; ^1H NMR (300 MHz, DMSO- d_6 , δ , ppm): 4.60 (1H, s, NHAr), 7.25 (4H, s, ArH), 8.01 (1H, s, =CH), 10.07 (2H, s, NHNH), 11.12 (2H, s, NHBA); ^{13}C NMR (300 MHz, DMSO- d_6 , δ , ppm) 177 (C=S thiamide), 163 (C=O amide), 140 (CBr benzene), 138 (CH ethylene), 131 (C benzene), 130 (CH benzene), 125 (CH benzene), 118 (CH benzene), 113 (CH benzene), 79 (C ethylene); EIMS (70 eV) m/z (%): ([M+/M+2], 400/402 (4/4)), 352 (61), 287 (10), 247 (4), 230 (6), 213/215 (100/94), 198 (18), 171 (48), 155 (22), 134 (22), 117 (20), 102 (5), 75 (11), 44 (17); (Found: C, 36.08; H, 2.53; N, 17.53; S, 16.03 %. Calc. For $\text{C}_{12}\text{H}_{10}\text{N}_5\text{O}_2\text{S}_2\text{Br}$: C, 36.09; H, 2.51; N, 17.54; S, 16.04 %).

N-[3-(trifluoromethyl)phenyl]-2-[(2,4,6-trioxotetrahydropyrimidin-5(2H)-ylidene)methyl] hydrazinecarbothioamide (**10**) Yield 88 % as mustard solid; m.p. 238 °C; ^1H NMR (300 MHz, DMSO- d_6 , δ , ppm): 4.41 (1H, s, NHAr), 7.38 (1H, s, ArH), 7.51 (3H, m, ArH), 8.12 (1H, s, =CH), 10.31 (2H, s, NHNH), 11.00 (2H, s, NHBA); ^{13}C NMR (300 MHz, DMSO- d_6 , δ , ppm) 197 (C=S thiamide), 167 (C=O amide), 154 (CH ethylene), 151(C benzene), 150 (CH benzene), 131 (CH benzene), 123 (CF₃), 99 (C

ethylene); EIMS (70 eV) m/z (%): ([M+], 373 (2)), 345 (5), 293 (20), 251 (5), 234 (10), 218 (2), 202 (20), 188 (23), 177 (23), 150 (31), 128 (15), 100 (15), 85 (9), 69 (17), 42 (14); (Found: C, 41.81; H, 2.67; N, 18.78, S, 8.59 %. Calc. For $C_{13}H_{10}N_5O_3SF_3$: C, 41.82; H, 2.68; N, 18.77; S, 8.58 %).

2-[(4,6-dioxo-2-thioxotetrahydropyrimidin-5(2H)-ylidene)methyl]-N-[4-(trifluoromethyl)phenyl]hydrazinecarbothioamide (**11**) Yield 91 % as yellow solid; m.p. 280 (dec.) °C; 1H NMR (300 MHz, DMSO- d_6 , δ , ppm): 4.37 (1H, s, NHAr), 7.37 (2H, d, J 9, ArH), 7.75 (2H, d, J 9, ArH), 8.00 (1H, s, =CH), 9.70 (2H, s, NHNH), 11.15 (1H, s, NHBA), 11.40 (1H, s, NHBA); ^{13}C NMR (300 MHz, DMSO- d_6 , δ , ppm) 192 (C=S thiamide), 163 (C=O amide), 121 (CH benzene), 120 (CH benzene), 118 (CF₃), 99 (C ethylene); EIMS (70 eV) m/z (%): ([M+], 389 (2)), 367 (5), 345 (5), 293 (20), 251 (5), 234 (10), 218 (2), 202 (20), 188 (23), 177 (23), 150 (31), 122 (15), 108 (15), 95 (9), 69 (17), 44 (14); (Found: C, 40.11; H, 2.58; N, 17.99; S, 16.47 %. Calc. For $C_{13}H_{10}N_5O_2S_2F_3$: C, 40.10; H, 2.59; N, 17.99; S, 16.45 %).

2-[(4,6-dioxo-2-thioxotetrahydropyrimidin-5(2H)-ylidene)methyl]-N-(4-methoxyphenyl)hydrazinecarbothioamide (**12**) Yield 91 % as yellow solid; m.p. 230 (dec.) °C; 1H NMR (300 MHz, DMSO- d_6 , δ , ppm): 3.75 (3H, s, OCH₃), 4.60 (1H, s, NHAr), 6.90 (2H, dd, J 3.9, ArH), 7.38 (2H, d, J 9, ArH), 9.53 (1H, s, =CH), 9.73 (2H, s, NHNH), 11.57 (2H, s, NHBA); ^{13}C NMR (300 MHz, DMSO- d_6 , δ , ppm) 198 (C=S thiamide), 163 (C=O amide), 156 (C benzene), 132 (CH ethylene), 131 (C benzene), 126 (CH benzene), 125 (CH benzene), 113 (C ethylene), 55 (OCH₃); EIMS (70 eV) m/z (%): ([M+], 351 (2)), 328 (70), 313 (27), 277 (3), 239 (48), 224 (8), 207 (2), 197 (61), 180 (6), 165 (100), 150 (90), 133 (22), 122 (52), 108 (46), 92 (8), 77 (11), 63 (8), 44 (4); (Found: C, 44.43; H, 3.73; N, 19.92; S, 18.22 %. Calc. For $C_{13}H_{13}N_5O_3S_2$: C, 44.44; H, 3.70; N, 19.94; S, 18.23 %).

N-(4-cyanophenyl)-2-[(2,4,6-trioxotetrahydropyrimidin-5(2H)-ylidene)methyl]hydrazine carbothioamide (**13**) Yield 94 % as whitish yellow solid; m.p. 228 °C; 1H NMR (300 MHz, DMSO- d_6 , δ , ppm): 4.91 (1H, s, NHAr), 7.32 (2H, d, J 9, ArH), 7.69 (2H, d, J 9, ArH), 8.24 (1H, s, =CH), 9.50 (2H, s, NHNH), 11.12 (2H, s, NHBA); ^{13}C NMR (300 MHz, DMSO- d_6 , δ , ppm): 179 (C=S thiamide), 167 (C=O amide), 151 (CH ethylene), 135 (C benzene), 128 (CH benzene), 126 (CN), 86 (C ethylene); EIMS (70 eV) m/z (%): ([M+], 330 (1)), 316 (18), 192 (41), 160 (100), 143 (42), 129 (28), 118 (33), 102 (25), 90 (11), 75

(20), 64 (7), 51 (7); (Found: C, 47.26; H, 3.04; N, 25.46; S, 9.72 %. Calc. For $C_{13}H_{10}N_6O_3S$: C, 47.27; H, 3.03; N, 25.45; S, 9.70 %).

Antibacterial activity (in vitro)

All the synthesized compounds were screened for their antibacterial activity against *E. coli*, *P. aeruginosa*, *S. typhi*, and *S. aureus*, by agar-well diffusion method (Olaleye, 2007). Nutrient agar plates were prepared by pouring 20–25 mL autoclaved nutrient agar into sterile plates and allowed to solidify. The plates were swabbed with 2–8-h-old bacterial inoculums containing approximately 10^4 – 10^6 colony forming units (CFU/mL) (already prepared and kept at 37 °C). The wells (6 mm in diameter) were dug in media with sterile metallic borer followed by the addition of 50 μ L of test solution (1 mg/mL in DMSO) into the respective wells. Other wells supplemented with DMSO and reference antibacterial drug, chloramphenicol, served as negative and positive controls, respectively. The plates were incubated at 37 °C for 24 h, after that the zone of inhibition around each well was measured using a transparent scale.

Minimum inhibitory concentration (MIC) values of these test samples were determined by “Micro-titer assay” as reported by (Sarker *et al.*, 2007) using 2,3,5-triphenyl-tetrazolium chloride (TTC) as indicator solution. For this a stock solution of concentrations 4,000, 2,000, 1,000, 500, 250, 125, 62.5, and 31.25 μ g/mL of each test compound and positive control (Chloramphenicol) was prepared in DMSO by serial dilution, while the bacterial culture was maintained in nutrient broth. Twenty microliters from each of the above-mentioned stock solutions was added into the respective well of 96-well plate followed by the addition of 180 μ L of bacterial suspension (10^8 CFU/mL) such that each test compound was checked at the final concentration of 400, 200, 100, 50, 25, 12.5, 6.25, and 3.12 μ g/mL. Controls were used on each plate, a broad spectrum antibiotic as positive control (Chloramphenicol), negative control (DMSO), and blank (bacterial suspension in nutrient broth). The plates were prepared in triplicate and incubated at 37 °C for 18–24 h. After incubation, to each well 20 μ L of TTC indicator solution (prepared as 5 mg/mL D-H₂O) was added, and plates were incubated again for 15–20 min. The change in color was then observed visually. Any color change toward pink indicated the presence of viable bacteria, while no change in color was considered as dead bacteria. The MIC values were taken as lowest concentration at which no color change appeared. Experiment was repeated three times and the average of three readings was taken as MIC for the test compound against a specific bacteria.

Cholinesterase inhibition assay (*in vitro*)

AChE and BChE inhibition activities were performed, with slight modifications, according to Ellman *et al.*, (1961). Total volume of the reaction mixture was raised to 100 by 60 μL Na_2HPO_4 buffer (of concentration 50 mM and pH 7.7) and 10 μL test compound (0.5 mM well^{-1}), followed by the addition of 10 μL ($0.005 \text{ unit well}^{-1}$) enzyme. After mixing the contents were pre-read at 405 nm and pre-incubated for 10 min at 37 °C. The addition of 10 μL of 0.5 mM well^{-1} substrate (acetyl thiocholine iodide/butyryl thiocholine iodide) initiated the reaction, followed by the addition of 10 μL DTNB (0.5 mM well^{-1}). Absorbance was measured, after 30 min of incubation at 405 nm and 37 °C, using Eserine (0.5 mM well^{-1}) as a positive control. Statistical analysis was performed using Microsoft Excel 2003, presenting results as mean \pm SEM. The formula used for calculating percent inhibition is as follows:

$$\text{Inhibition (\%)} = \frac{\text{Control} - \text{test}}{\text{Control}} \times 100.$$

Concentration at which there is 50 % enzyme inhibition (IC_{50}) of compounds was calculated using EZ-Fit Enzyme kinetics software (Perella Scientific Inc. Amherst, USA). All the measurements were done in triplicate using Synergy HT (BioTek, USA) 96-well plate reader.

Molecular docking protocol

Human AChE and BChE crystal structures (with PDB accession codes of 1B41 and 2WID, respectively) were retrieved from the Protein Data Bank (PDB). UCSF Chimera 1.6.1 was used to reconstruct missing residues (from 465 to 470) found in the crystal structure of AChE, whereas crystal structure of BChE was allowed to align with another PDB file of human (PDB accession code, 1POP) in order to reconstruct missing residues (Kryger *et al.*, 2000; Pettersen *et al.*, 2004). Visual Molecular Dynamics, VMD 1.9 (William *et al.*, 1996) was used to remove water molecules from the crystal structures of both proteins. Structures of newly synthesized compounds were docked against receptor sites of crystal structures of AChE and BChE. All the structures were built in 3D-PDB format followed by geometry optimization at RM1 semi-empirical level of theory by the programs Gabedit (Allouche, 2010) and MOPAC 2012 (Stewart, 2007), respectively. Docking studies were carried out by AutoDock Vina (Trott and Olson, 2010), using built-in Lamarckian genetic algorithm method. A total of 20 runs were performed for each docking, and the rest of the parameters were set to default values.

Search space was restricted to a grid box size of $46 \times 46 \times 46$ in x , y , and z dimensions, respectively, centered on the binding site of protein with x , y , and z coordinates

of 120.491, 106.059, and -136.443 \AA , respectively. All the docking runs were performed on Intel(R) Core(TM) i5-2410M CPU @ 2.30 GHz of Sony origin, with 6.0 GB DDR RAM. AutoDock Vina was compiled and run under Windows 7 Professional 64-bit operating system.

Acknowledgments One of the authors Saira Mumtaz likes to thanks Higher Education Commission of Pakistan for providing funding and support throughout this study.

References

- Allderdice PW, Garner HAR, Galutira D, Lockridge O, LaDu BN, McAlpines J (1991) The cloned butyrylcholinesterase (BChE) gene maps to a single chromosome site. *Genomics* 11:452–454
- Allouche AR (2010) Gabedit—a graphical user interface for computational chemistry softwares. *J Comput Chem* 32(1):174
- Andrade CH, Pasqualoto FMK, Ferreira IE, Hopfinger NJ (2010) 4D-QSAR: perspectives in drug design. *J Mol* 15:3281
- Chatonnet A, Lockridge O (1989) Comparison of butyrylcholinesterase and acetylcholinesterase. *J Biochem* 260:625–634
- Ekholm M (2001) Predicting relative binding free energies as substrate and inhibitors of acetyl- and butyryl cholinesterase. *Theo chem* 572:25–34
- Ellman GL, Courtney KD, Andres V, Featherstone RM (1961) A new and rapid colorimetric determination of acetylcholinesterase activity. *J Biochem Pharmacol* 7:88–95
- Gilman AG, Rall TW, Nies A, Taylor P (1990) The pharmacological basis of therapeutics. Pergamon, New York 131
- Hallak M, Giacobini E (1989) Physostigmine, tacrine and metrifonate—the effect of multiple doses on acetylcholine metabolism in rat brain. *Neuropharmacology* 28:199–206
- Hucho F, Jam J, Weise C (1991) Substrate-binding sites in acetylcholinesterase. *Trends Pharmacol Sci* 12:422–426
- Khan KM, Ali M, Wadood A, Zaheer-ul-Haq, Khan M, Lodhi MA, Perveen S, Choudhary MI, Voelter W (2011) Molecular modeling-based antioxidant arylidene barbiturates as urease inhibitors. *J Mol Graph Model* 30:153–156
- Kryger G, Harel M, Giles K, Tokar L, Velan B, Lazar A, Kronman C, Barak D, Ariel N, Shafferman A, Silman I, Sussman JL (2000) Structures of recombinant native and E202Q mutant human acetylcholinesterase complexed with the snake-venom toxin fasciculin-II. *Acta Crystallogr D* 56:1385–1394
- Mihai VP, Diana J, Chiriac A, Ienciu L (2008) Molecular modeling of barbiturates. *Ann West Univ Timisoara Ser Chem* 17(3):45–50
- Olaleye MT (2007) Cytotoxicity and antibacterial activity of methanolic extract of Hibiscus sabdariffa. *J Med Plants Res* 1:9–13
- Pan D, Tseng Y, Hopfinger AJ (2003) Quantitative structure-based design: formalism and application of receptor-dependent RD-4D-QSAR analysis to a set of glucose analogues inhibitors of glycogen phosphorylase. *J Chem Inf Comput Sci* 43:1591–1607
- Pettersen EF, Goddard TD, Huang CC, Couch GS, Greenblatt DM, Meng EC, Ferrin TE (2004) UCSF chimera—a visualization system for exploratory research and analysis. *J Comput Chem* 25:1605–1612
- Quinn D (1987) Acetylcholinesterase: enzyme structure, reaction dynamics, and virtual transition states. *Chem Rev* 87:955–979
- Rauf A, McNab H, Qureshi AM (2012) An efficient one pot three component synthesis of *N*-(methylene-4-oxocoumarinyl) anilines; their Z, E-Isomeric product distribution determination from ^1H NMR and their antibacterial studies. *Lett Drug Des Discov* 9(5):454–458

- Ryhänen RJJ (1983) Pseudocholinesterase activity in some human body fluids. *Gen Pharmacol* 14:459–460
- Santos-Filho OA, Hopfinger AJ (2006) Structure-based QSAR analysis of a set 4-hydroxy-5,6-dihydropyrones as inhibitors of HIV-1 protease: an application of the receptor-dependent (RD) 4D-QSAR formalism. *J Chem Inf Model* 46:345
- Sarker SD, Nahar L, Kumarasamy Y (2007) Microtiter plate-based antibacterial assay incorporating resazurin as an indicator of cell growth, and its application in the in vitro antibacterial screening of phytochemicals. *Methods* 42:321–324
- Stewart JP (2007) Optimization of parameters for semiempirical methods V: modification of NDDO approximations and application to 70 elements. *J Mol Model* 13:1173
- Sussman LJ, Harel M, Frolow F, Oefner C, Goldman A, Toker L, Silman I (1991) Atomic structure of acetylcholinesterase from *Torpedo californica*: a prototypic acetylcholine-binding protein. *Science* 253:872–879
- Trott O, Olson AJ (2010) AutoDock Vina: improving the speed and accuracy of docking with a new scoring function, efficient optimization and multithreading. *J Comput Chem* 31(2):455
- William H, Andrew D, Klaus S (1996) VMD-visual molecular dynamics. *J Mol Graph* 14:33–38